J Mol Model (2012) 18:3213–3217
DOI 10.1007/s00894-011-1343-6

ORIGINAL PAPER

Density functional studies on the endohedral complex of fullerene C_{70} with tetrahedrane (C_4H_4): $C_4H_4@C_{70}$

Xiao-Yuan Ren · Cai-Ying Jiang

Received: 27 June 2011 / Accepted: 19 December 2011 / Published online: 14 January 2012

Abstract B3LYP/6-31G(d) hybrid HF/DFT calculations were carried out to determine the structural and electronic properties of the endohedral complex of a C_{70} cage with tetrahedrane (C_4H_4). It was demonstrated that the formation of the complex is endothermic, with a destabilization energy of 72.56 kcal mol^{-1}. C_4H_4 is seated in the center of the C_{70} cage and exists in molecular form inside the fullerene. C_4H_4 endohedral doping slightly perturbs the molecular orbitals of C_{70}. The calculated HOMO–LUMO gaps, the electron affinity (EA), and the ionization potential (IP) indicate that $C_4H_4@C_{70}$ is more chemically reactive than C_{70}. The IR active modes and harmonic vibrational frequencies of $C_4H_4@$ C_{70} are also discussed.

Keywords Quantum chemistry · Density functional method · Endohedral fullerene · Electronic spectrum

Introductions

At the time of the discovery of C_{60} by Kroto et al. [1] in 1985, endohedral fullerenes had already been suggested, based on mass spectroscopic results [2]. As fullerenes have spherical nanometer-scale empty spaces inside their carbon cages, it is an intuitively natural idea to try to stuff atoms or small molecule into this void [3–5]. Such endohedral fullerene molecules with imcorporated impurities should have quite different physical and chemical properties to the corresponding pristine molecules, and these properties can potentially be exploited for various purposes, from molecular electronics to biomedical applications. Both experimental and theoretical research has revealed that the chemical and physical properties of endohedral fullerenes can be fine-tuned through the appropriate selection of both the fullerene cage and the encaged atom or small molecule [5–8]. In our previous paper [9], we described theoretical calculations we performed that focused on the endohedral complex of fullerene C_{60} with tetrahedrane, i.e., $C_4H_4@C_{60}$. It was demonstrated that C_4H_4 was seated in the center of the C_{60} cage and existed in a molecular form inside the fullerene. The formation of this complex was endothermic. C_4H_4 endohedral doping slightly perturbed the molecular orbitals of C_{60}. The calculated HOMO–LUMO gaps, the electron affinity (EA), and the ionization potential (IP) indicated that $C_4H_4@C_{60}$ is more chemically reactive than C_{60}.

Aside from its more famous cousin C_{60}, C_{70} is the most abundant product resulting from the macroscopic production of fullerenes. Its structure is obtained from that of C_{60} by adding a ring of hexagons along an equatorial line. In contrast to the C_{60} molecule with its I_h symmetry, the C_{70} molecule has a lower level of symmetry, D_{5h}, and lacks inversion symmetry—it is not spherical; it has a slightly elongated rugby-ball shape. Owing to its elongated form and reduced symmetry, the electronic, vibrational, and dynamic properties of C_{70} differ from those of C_{60}. On the other hand, due to the insertion of ten additional atoms, fullerene C_{70} has a relatively large and robust cage, which promises a wide range of applications upon filling it with atoms or molecules. Here, we report our studies on the

X.-Y. Ren (✉) · C.-Y. Jiang
College of Life Sciences, Zhejiang Sci-Tech University,
Hangzhou 310018, China
e-mail: pine_ren@yahoo.com.cn

endohedral complex of C_{70} with the tetrahedrane C_4H_4. The purposes of this paper are to report on the structural and electronic properties of $C_4H_4@C_{70}$, and to discuss the similarities and differences between $C_4H_4@C_{60}$ and $C_4H_4@C_{70}$. We hope that the present study will encourage further theoretical and experimental analysis of this system.

Computational details

Given the size of the system of interest, we performed calculations at the Hartree–Fock and DFT/B3LYP levels of theory with the STO-3G and 6-31G(d) basis sets for full geometry optimization and total energy calculation. Three models—HF/STO-3G, HF/6-31G(d), and B3LYP/6-31G (d)—were used in this sequence to obtain results at different levels of theory, as well as to minimize the computational cost. To ensure that true stationary points had been found, harmonic vibrational frequencies were also calculated by analytically evaluating the second derivative of the energy with respect to nuclear displacement. The B3LYP functional was chosen because including electron correlation was important for accurately predicting the geometry. Our experience of theoretical calculations on C_{60}-related derivatives also indicate that DFT is a very successful method for studying fullerene compounds [9–14]. All calculations were carried out with Hyperchem 7.5 [15] and the GAUSSIAN 03 software package [16], executed on a SGI Onyx3900 workstation, and the SCF was converged to 10^{-6} in both energy and density.

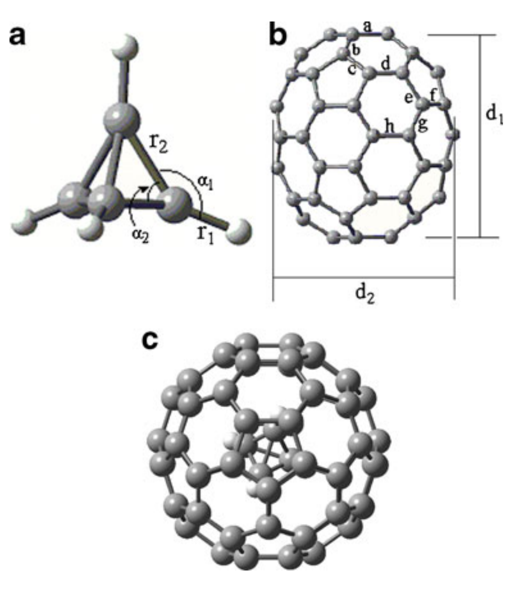

Fig. 1 B3LYP/6-31G(d) hybrid HF/DFT optimized geometries: **a** C_4H_4, **b** C_{70}, **c** $C_4H_4@C_{70}$ (C_s)

Table 1 B3LYP/6-31G(d) optimized geometry parameters (bond lengths in Å and bond angles in degrees)

	C_4H_4	C_{70}(DFT)	$C_4H_4@C_{70}$(DFT)
r_1	1.073	-	1.057
r_2	1.480	-	1.416–1.592
α_1	144.7	-	116.07–143.20
α_2	60.0	-	55.77–68.34
r_a	-	1.452	1.449–1.457
r_b	-	1.397	1.394–1.403
r_c	-	1.448	1.450–1.456
r_d	-	1.388	1.392–1.401
r_e	-	1.449	1.448–1.460
r_f	-	1.434	1.441–1.447
r_g	-	1.421	1.420–1.430
r_h	-	1.472	1.483–1.484
d_1	-	7.938	7.905
d_2	-	7.088	7.158

Results and discussion

The B3LYP/6-31G(d) optimized geometries are shown in Fig. 1. Some geometry parameters are listed in Table 1. The C_{70} cage, with its rugby-ball shape and D_{5h} symmetry, has 105 C–C bonds, which can be classified into eight types: 10 “a” bonds, 10“b,” 20 “c,” 10 “d,” 20 “e,” 10 “f,” 20 “g,” and 5 “h” bonds. The free C_{70} molecule was first calculated at the HF/STO-3G level (lowest frequency: 253.24 cm^{-1}) and finally at the B3LYP/6-31G(d) level, which gave the following bond lengths: r_a = 1.452 Å, r_b=1.397 Å, r_c=1.448 Å, r_d = 1.388 Å, r_e=1.449 Å, r_f=1.434 Å, r_g=1.421 Å, r_h=1.472 Å. The overall dimensions of the cage, taken to be the distance between corresponding carbon atoms in the five-membered rings in the two caps (d_1) and the distance between the two farthest separated atoms on the equator (d_2), are also listed. This result is consistent with previous calculations and experimental results [17, 18].

The energy minima of $C_4H_4@C_{70}$ were found by performing full geometry optimization without symmetry limitations at the HF/STO-3G level of theory (lowest frequency: 71.81 cm^{-1}) and finally at the B3LYP/6-31G(d) level, which yielded the complex geometries shown in Fig. 1. Some geometric parameters are listed in Table 1. The T_d C_4H_4 is seated in the center of the fullerene cage, and the D_{5h} symmetry of the cage is reduced to C_s for the endohedral complex. Both the encaged tetrahedrane and the C_{70} cage are extremely distorted. The C_{70} cage is shortened by about 0.04 Å longitudinally and elongated by about 0.07 Å latitudinally. The C–H bonds of the encaged tetrahedrane C_4H_4 are shortened, but C–C bonds perpendicular to or in the σ_h plane are elongated (the others are shortened). The C–C–H bond angles are also somewhat distorted. The deformations in the bond lengths, bond angles, and twist angles of neighboring carbon atoms thus lead to symmetry-reducing distortions of the cage. The distances between the H and the C atoms in C_4H_4 and the nearest C atoms in C_{70} are 2.096 and 2.859 Å, respectively, implying that the encapsulated T_d C_4H_4 only exists in a molecular form inside the fullerene; it is not adsorbed onto the internal surface of the carbon structure.

Mulliken population analysis showed that electronic charge transfer occurs from the C_{70} cage to the C_4H_4 in $C_4H_4@C_{70}$. As listed in Table 2, the central guest C_4H_4 gains negative charge (−0.062) from the cage. This electronic charge transfer is weaker than in $C_4H_4@C_{60}$, where the guest C_4H_4 gains −0.257 of negative charge [9]. With either a C_{70} or C_{60} fullerene cage acting as an electron-donating substituent [19], it appears that the highly strained C_4H_4 may be stabilized in the fullerene cage due to the accumulation of negative charge on the skeleton.

The molecular orbitals of C_{70} are not perturbed by C_4H_4 endohedral doping as much as those of C_{60} are. Table 2 shows that $C_4H_4@C_{70}$ has a smaller HOMO–LUMO gap than C_{70}, which indicates that the inclusion of C_4H_4 can make the fullerene cage more reactive. Relative to C_{70}, the molecular orbital levels of $C_4H_4@C_{70}$ are perturbed by the inclusion of the tetrahedrane, and the degenerate energy levels are split. Figure 2 displays the electronic levels near the HOMO–LUMO energy gap obtained from B3LYP/6-31G(d) level calculations. Compared with C_{70}, the HOMO of $C_4H_4@C_{70}$ is slightly higher (by 0.37 eV) and the LUMO is slightly lower (by 0.05 eV). There is an obvious reduction in electronic level degeneracy for $C_4H_4@C_{70}$. The LUMOs are two degenerate orbitals and the HOMO is one orbital. The energy gap between the HOMO and LUMO levels is 2.27 eV: 0.42 eV less than the 2.69 eV of C_{70} and 0.17 eV more than the 2.10 eV of $C_4H_4@C_{60}$. This result indicates that $C_4H_4@C_{70}$ is more chemically reactive than C_{70} and less reactive than $C_4H_4@C_{60}$ [20–22].

The electron affinity (EA) and ionization potential (IP) of $C_4H_4@C_{70}$ calculated at the B3LYP/6-31G(d)/B3LYP/6-31G (d) level were found to be 3.28 and 5.55 eV, respectively. Considering the values of 3.23 and 5.92 eV calculated at the same level of theory for C_{70}, it is more probable that $C_4H_4@C_{70}$ will accept or donate electrons due to its enhanced EA and reduced IP values. Thus, $C_4H_4@C_{70}$ is more chemically reactive than C_{70}, as suggested by the abovementioned HOMO–LUMO gaps [20–22]. In order to gain insight into the HOMO and LUMO properties of $C_4H_4@C_{70}$, we plotted the probability density contours of the two levels. As shown in Fig. 3, the HOMO and LUMO were found to be localized on the carbon cage, thus suggesting the reactive sites of this compound.

To assess relative stabilities, binding energies (BE) were calculated according to the gas-phase reaction $nX+mY=X_nY_m$. This means that $BE(X_nY_m)=E(X_nY_m) - nE(X) - mE(Y)$, and a more thermodynamically stable species should have a more negative BE. The inclusion energy (E_{inclu}) of the endohedral complex was also evaluated by comparing the energy of $C_4H_4@C_{70}$ to the sum of the energies of the isolated components T_d C_4H_4 and C_{70}; that is, $E_{inclu}=E(C_4H_4@C_{70}) - [E(C_4H_4)+E(C_{70})]$. Our results obtained at the B3LYP/6-31G (d)//B3LYP/6-31G(d) level indicated that the formation of $C_4H_4@C_{70}$ from the free molecules T_d C_4H_4 and C_{70} is more energetically favorable (inclusion energy: 72.56 kcal mol^{-1}) than the formation of $C_4H_4@C_{60}$ from its corresponding free molecules (141.05 kcal mol^{-1}). The binding energy of $C_4H_4@C_{70}$ is −12047.75 kcal mol^{-1}, which is more negative than the binding energy, −10304.93 kcal mol^{-1}, of $C_4H_4@C_{60}$. These calculated values for the inclusion energy and binding energy suggest that $C_4H_4@C_{70}$ is more stable than $C_4H_4@C_{60}$, and that larger fullerenes enable the endohedral species to be manipulated with greater ease. $C_4H_4@C_{70}$ may exist as a

Table 2 Results of B3LYP/6–31G(d)//B3LYP/6–31G(d) calculations

	Charges on C_4H_4		Total dipole moment (Debye)	$\Delta E_{HOMO-LUMO}$ (eV)	Total energies (au)
C_4H_4	C_1 −0.144	H_1 0.144	0	−9.25	−154.636686560
	C_2 −0.144	H_2 0.144			
	C_3 −0.144	H_3 0.144			
	C_4 −0.144	H_4 0.144			
C_{70}			0	−2.69	−2667.30410639
$C_4H_4@C_{70}$	C_1 −0.133	H_1 0.123	0.0637	−2.27	−2821.82516024
	C_2 −0.152	H_2 0.127			
	C_3 −0.133	H_3 0.123			
	C_4 −0.145	H_4 0.128			

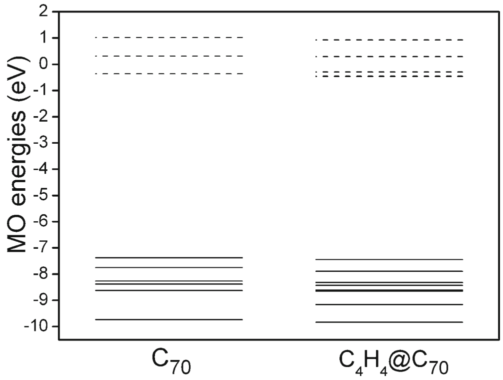

Fig. 2 Electronic energy levels of C_{70} and $C_4H_4@C_{70}$ near the HOMO–LUMO gap obtained at BLYP/6-31G(d); *solid lines* and *dashed lines* refer to occupied and unoccupied states, respectively

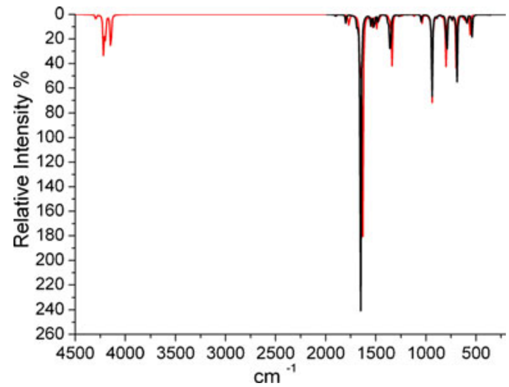

Fig. 4 Calculated IR spectra of $C_4H_4@C_{70}$ (*red line*) and C_{70} (*solid line*)

stable species, and although rigorous conditions are needed to synthesize this compound, experimental attempts in this direction should be rewarding.

Our calculation at the HF/STO-3G level of theory indicated that there are 47 infrared-active modes in $C_4H_4@C_{70}$. The harmonic vibrational frequencies and intensities of these modes are: 515 (1), 559 (17), 594 (4), 595 (3), 620 (2), 698 (23), 700 (22), 741 (2), 793 (2), 801 (24), 802 (23), 815 (1), 933 (1), 936 (4), 940 (36), 941 (34), 967 (1), 1038 (4), 1040 (3), 1245 (1), 1340 (41), 1351 (2), 1351 (1), 1363 (1), 1364 (2), 1465 (3), 1467 (3), 1488 (5), 1490 (6), 1533 (7), 1533 (6), 1538 (2), 1629 (100), 1632 (94), 1651 (20), 1653 (4), 1656 (30), 1656 (5), 1663 (4), 1665 (3), 1765 (6), 1768 (4), 1776 (2), 4145 (43), 4197 (22), 4217 (43), 4295 (5); note that IR intensities (in km mol^{-1}) of the active modes are given in parentheses. The strongest band, with an intensity of 100 km mol^{-1}, is associated with the highest frequency mode, at 1629 cm^{-1}. This normal mode mainly corresponds to C–C stretches of the host C_{70} cage perpendicular to the σ_h plane. A complete list of all vibrational modes (a total of 228) is available on request from the corresponding author. The calculated spectrum of $C_4H_4@C_{70}$ is shown in Fig. 4; for comparison, the spectra of C_{70} and $C_4H_4@C_{60}$ calculated at the same level of theory are also shown. There is a large redshift in the most intense vibration in the spectrum of $C_4H_4@C_{70}$ when compared with that of $C_4H_4@C_{60}$.

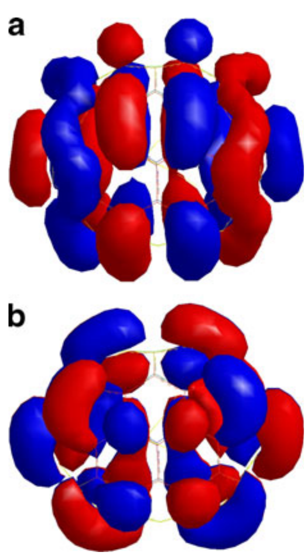

Fig. 3 Isodensity surfaces (0.01 e/au^3) associated with $C_4H_4@C_{70}$, obtained via Hartree–Fock calculations: **a** HOMO and **b** LUMO

Summary

We have studied the structural and electronic properties of $C_4H_4@C_{70}$ at the Hartree–Fock self-consistent field (SCF) and density-functional B3LYP levels of theory using the STO-3G and 6-31G(d) basis sets. The T_d C_4H_4 is seated in the center of the C_{70} cage, and the D_{5h} symmetry of the cage is reduced to C_s for $C_4H_4@C_{70}$. Both the fullerene cage and the encaged tetrahedrane experience considerable structural changes. However, the encapsulated C_4H_4 only exists in a molecular form inside the fullerene; it is not adsorbed onto the internal surface of the carbon structure. The calculated results for the inclusion energy and binding energy indicate that $C_4H_4@C_{70}$ is more stable than $C_4H_4@C_{60}$. The calculated HOMO–LUMO gaps as well as the EA and the IP values have also been presented as indicators of chemical stability. There are 47 infrared-active modes in $C_4H_4@C_{70}$, and there is a large redshift in the most intense vibration in the spectrum of $C_4H_4@C_{70}$ when compared with that of $C_4H_4@C_{60}$. The molecular properties calculated for this compound may prove valuable in future experimental research.

Acknowledgments This work is supported by the Science Foundation of Zhejiang Sci-Tech University (ZSTU; grant no. 0816833-Y) and the Zhejiang Provincial Natural Science Foundation of China (grant no. Y304122).

References

1. Kroto HW, Heath JR, O'Brien SC, Curl RF, Smalley RE (1985) C_{60}: buckminsterfullerene. Nature 318:162–163
2. Heath JR, Brien SC, Zhang Q, Liu Y, Curl RF, Kroto HW, Tittel FK, Smalley RE (1985) Lanthanum complexes of spheroidal carbon shells. J Am Chem Soc 107:7779–7780
3. Shinohara H (2000) Endohedral metallofullerenes. Rep Prog Phys 63:843–892
4. Shiotani H, Ito T, Iwasa Y, Taninaka A, Shinohara H, Nishibori E, Takata M, Sakata M (2004) Quantum chemical study on the configurations of encapsulated metal ions and the molecular vibration modes in endohedral dimetallofullerene $La_2@C_{80}$. J Am Chem Soc 126:364–369
5. Murata M, Murata Y, Komatsu K (2006) Synthesis and properties of endohedral C_{60} encapsulating molecular hydrogen. J Am Chem Soc 128:8024–8033
6. Johnson RD, de Vries MS, Salem J, Bethune DS, Yannoni CS (1992) Electron paramagnetic resonance studies of lanthanum-containing C_{82}. Nature 355:239–240
7. Laasonen K, Andreoni W, Parrinello M (1992) Structural and electronic properties of $La@C_{82}$. Science 258:1916–1917
8. Nagase S, Kobayashi K (1993) A theoretical approach to C_{82} and LaC_{82}. Chem Phys Lett 201:475–480
9. Ren XY, Jiang CY, Wang J, Liu ZY (2008) Endohedral complex of fullerene C_{60} with tetrahedrane, $C_4H_4@C_{60}$. J Mol Graph Model 275:558–562
10. Ren XY, Liu ZY (2005) Structural and electronic properties of S-doped fullerene C_{58}, where is the S atom situated? J Chem Phys 122:034306
11. Ren XY, Liu ZY, Zhu MQ, Zheng KL (2004) DFT studies on endohedral fullerene $C@C_{60}$, C centers the C_{60} cage. J Mol Struct (THEOCHEM) 710:175–178
12. Ren XY, Liu ZY (2005) Endohedral complex of fullerene C_{60} with tetrahedral N_4, $N_4@C_{60}$. Struct Chem 16:567–570
13. Ren XY, Liu ZY, Guo XH (2004) Gas-phase synthesis and the structural and electronic properties of $C_{60}S^+$ studied by mass spectrometry and molecular orbital calculation. J Mol Struct (THEOCHEM) 686:43–46
14. Ren XY, Liu ZY (2007) Structural and electron properties of the highest epoxygenated $C_{60}O_{30}$, a DFT study. J Mol Graph Model 26:336–341
15. Hypercube Inc. (2002) Hyperchem, release 7.5. Hypercube Inc., Fainesville
16. Frisch MJ et al (2004) Gaussian 03, revision C.02. Gaussian Inc., Wallingford
17. Sun G, Kertesz M (2002) Vibrational Raman spectra of C_{70} and C_{70}^{6-} studied by density functional theory. J Phys Chem A 106:6381–6386
18. Nikolaev AV, Dennis TJ, Prassides K, Soper AK (1994) Molecular structure of the C_{70} fullerene. Chem Phys Lett 223:143–148
19. Novak I (2003) Substituent effects on steric strain. Chem Phys Lett 380:258–262
20. Manolopoulos DE, May JC, Down SE (1991) Theoretical studies of the fullerenes: C_{34} to C_{70}. Chem Phys Lett 181:105–111
21. Liu X, Schmalz TG, Klein DJ (1992) Favorable structures for higher fullerenes. Chem Phys Lett 188:550–554
22. Diener MD, Alford JM (1998) Isolation and properties of small-bandgap fullerenes. Nature 393:668–671